Compartmental modeling of skin transport

A.A. Amarah[1,2], D.G. Petlin[1,3], J.E. Grice[4], J. Hadgraft[5], M.S. Roberts[4,6], Y.G. Anissimov[1,7*]

[1]School of Environment and Science, Griffith University, Gold Coast, Queensland, 4222, Australia

[2] University of Basrah, College of Science, Physics Department, Basrah, Iraq

[3]Tomsk Polytechnic University, 30 Lenin Avenue, Tomsk 634050, Russian Federation

[4]Therapeutics Research Centre, The University of Queensland Diamantina Institute, Translational Research Institute, Brisbane, 4102, Australia

[5]UCL School of Pharmacy, 29-39 Brunswick Square, London WC1N 1AX, United Kingdom

[6]Sansom Institute, School of Pharmacy and Medical Sciences, University of South Australia, Adelaide, SA, Australia

[7]Institute of Molecular Medicine, Sechenov First Moscow State Medical University, Moscow, Russia

* Correspondence: email: y.anissimov@griffith.edu.au, phone: +617 55528496

Abstract

The primary objective of this study is to introduce a simple and flexible mathematical approach which models transport processes in skin using compartments. The main feature of the presented approach is that the rate constants for exchange between compartments are derived from physiologically relevant diffusional transport parameters. This allows for better physical interpretation of the rate constants, and limits the number of parameters for the compartmental model. The resulting compartmental solution is in good agreement with previously published solutions for the diffusion model of skin when ten or more compartments are used. It was found that the new compartmental model with three compartments provided a better fit of the previously publish water penetration data than the diffusion model. Two special cases for which it is difficult to implement the diffusion model were considered using our compartmental approach. In both cases the compartmental model predictions agreed well with the diffusion model.

Introduction

Over the past decades, researchers have made significant efforts to better understand the skin and its functionalities. Morphologically, the skin is the largest organ with an area of approximately 2 m^2 providing a natural barrier between the body and surrounding environment. Further, skin contributes to around 10% of the total body mass, and researchers have found that human skin is composed of 3-4 main layers [1, 2]. These layers are arranged from the outer to the inner layers as follows: stratum corneum (SC), viable epidermis, dermis, and subcutaneous tissues [1, 2]. One of the important properties of skin is its permeability which plays a critical role for development of new transdermal drug delivery systems (TDDS).

Consequently, the understanding of drug transport from a TDDS into and through skin is crucial to the development of such systems, in order to achieve an optimal therapeutic effect [3]. Mathematical modeling of skin permeability is an important tool that can aid in the understanding of permeation mechanisms in dermal regions [4-6]. For example, modeling can help to predict the rate of penetration of drugs, as well as appropriate doses, exposure times, or sampling intervals. However, the validity of a mathematical model is largely dependent upon its capacity to predict experimental observations well [7].

A considerable amount of literature has been published on mathematical models of drug permeability through skin. Fick's first law deals with steady state diffusion phenomena and is used to predict exposure to TDDS over long time periods, when depletion in the system is not a significant factor [6]. In contrast, non–steady state diffusion can be analyzed by using Fick's second law which is based on a time dependent approach [8]. Furthermore, mathematical models can be applied in transdermal drug delivery simulation to predict the effects of dermal exposure to external elements, as well as to analyze percutaneous absorption kinetics and kinematics of bio-transport phenomena [9-11]. These models can be developed to mathematically represent diffusional processes in the SC as either a continuum, or as a series of discrete compartments [12-14]. As a result, physiological complexities of the SC can be considerably reduced by adopting the compartmental technique [11]. In this approach, the skin is treated as a number of well-stirred compartments, each of which have uniformly distributed solute concentration.

Compartmental or pharmacokinetic models (PK) are often used to describe the transport phenomena of material in biological systems, where compartments may represent different

sections of the body [15]. General mathematical approaches for compartmental models have been discussed in detail in the literature [16-18] and used for modelling drugs transport in skin [19, 20]. The compartmentalization of biological systems can aid in the elimination of space dependence in the mathematical formalism of the diffusion equation, which is generally a parabolic partial differential equation (PDE) [21]. As a result, a set of ordinary differential equations (ODEs) can be used to simulate transport processes in the transdermal drug delivery system instead of the PDE approach. Solving a set of ODEs is less computationally demanding than solving parabolic diffusion PDEs. Therefore, mathematical formalism of the compartmental system depends on the set of rate equations represented by ODEs [22]. In many instances, when rate coefficients are constant, the associated differential equations can be solved by Laplace transforms, but applying a numerical ODE solver is a more flexible and practical approach when using compartmental models.

In this paper, we derived ODEs to simulate skin transport processes in a finite volume donor using a compartmental approach. We then demonstrated that the predicted flux and receptor concentrations using the compartmental approach were close to corresponding values for the previously published diffusion models [23, 24]. Although skin structural complexities and different types of exposure scenarios exist, they can be easily implemented in the compartmental approach. To illustrate the flexibility of our approach, two different cases were considered: i), when the diffusion coefficient is a function of concentration and ii), when the donor volume is reducing due to evaporation. Using the diffusion model in these cases necessitates a relatively complex numerical approach such as the finite difference method. However, the new compartmental model allows for simpler numerical solutions which are based on the application of standard ODE solvers and give accurate results when compared to the numerical solutions of the diffusion model.

Theory

Anissimov and Roberts have used a diffusion model to theoretically describe two important cases of percutaneous absorption of a solute; firstly, when donor concentration is constant [23]; and secondly, when donor volume is finite [24]. In these works, models were developed to include such processes as donor-SC interfacial resistance, viable epidermal resistance, and clearance limitations in the receptor compartment. The Laplace transform technique was used for a wide variety of exposure scenarios of percutaneous penetration modeling [25-28]. However, this approach has significant limitations and cannot be applied when nonlinearities in the diffusion equation or time dependency in its coefficients are present [6, 29].

Zatz has developed a five compartments model of skin in which the rate constants are "analogous" to the diffusion coefficient of stratum corneum [4]. Hadgraft later used a similar approach to check the validity of the tape stripping technique for prediction of the steady state flux through the skin [30]. The compartmental approach was further formalized and compared to the diffusion model by considering how the number of compartments influences the precision of the model [10]. For a constant donor concentration, ten compartments were found to provide sufficient accuracy [10]. In the present work, the compartmental approach is extended to cover situations previously addressed only within the framework of the diffusion model [23, 24].
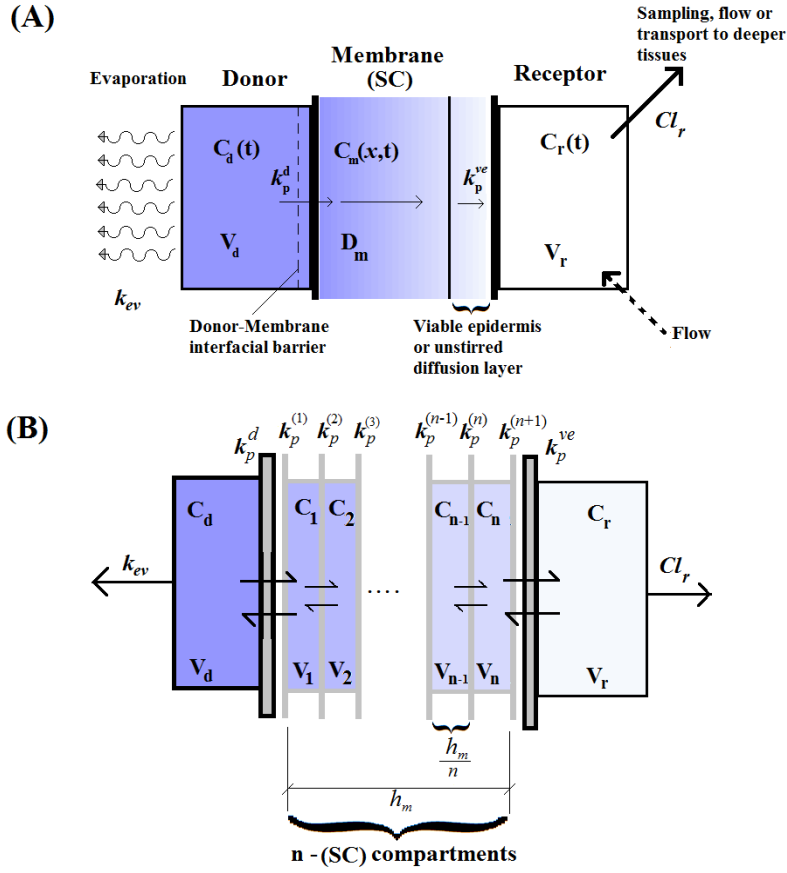
Figure 1. (A) Schematic diagram of the diffusion model, and (B) the corresponding compartmental model for the constant donor concentration, and the finite vehicle volume systems applied on membrane (SC).

Fig. 1 schematically illustrates the diffusional and the compartmental approaches. Generally, solute transport through the SC is assumed to be approximately described by a one dimensional diffusion equation [31]:

$$\frac{\partial C_m(x,t)}{\partial t} = D_m \frac{\partial^2 C_m(x,t)}{\partial x^2}$$

(1)

where D_m is the diffusion coefficient, $C_m(x,t)$ is the concentration of solute in the membrane as a function of distance (x) and time (t). At the beginning $(t=0)$, it is assumed that no solute is present in the membrane and therefore the initial condition is:

$$C_m(x,0) = 0$$

(2)

A second order space derivative in Equation (1) imposes two boundary conditions. The boundary conditions are illustrated in Fig. 1A. Firstly, at the donor surface $(x = 0)$ it is given as [23, 24]:

$$-D_m \frac{\partial C_m(x,t)}{\partial x}\bigg|_{x=0} = k_p^d \left(C_d(t) - \frac{C_m(0,t)}{K_m} \right)$$

(3)

Secondly, the boundary condition at the receptor surface $(x = h_m)$ is:

$$-D_m \frac{\partial C_m(x,t)}{\partial x}\bigg|_{x=h_m} = k_p^{ve} \left(\frac{C_m(h_m,t)}{K_m} - \frac{C_r(t)}{K_r} \right)$$

(4)

where $C_d(t)$ and $C_r(t)$ are the concentrations in the donor and receptor phase, respectively, which are defined as:

$$V_d \frac{dC_d}{dt} = AD_m \frac{\partial C_m(x,t)}{\partial x}\bigg|_{x=0} - Cl_{ev}C_d(t)$$

(5)

$$V_r \frac{dC_r}{dt} = -AD_m \frac{\partial C_m(x,t)}{\partial x}\bigg|_{x=h_m} - Cl_r C_r(t)$$

(6)

where h_m is the total membrane thickness, K_m, K_r are the partition coefficients between donor-membrane, and donor-receptor. k_p^d, k_p^{ve} are the permeability coefficients of donor, and viable epidermis layers interface, V_d, V_r are the volume of donor and receptor respectively, Cl_{ev} is the clearance from the donor phase due to the evaporation of the solute, and Cl_r is the removal rate of solution containing solute from the receptor phase.

We aimed to introduce the compartmental model that approximates Equation (1) with the rate constants related to physiological parameters. The permeability coefficient k_p is often used to describe diffusion of a solute across biological membranes [32]. Fig. 1B shows a diagrammatical representation of the compartmental model, in which the SC is transformed into a chain of n compartments that are separated by $n+1$ sub-membranes with individual

permeability coefficients $k_p^{(i)}$. Based on this scheme and the conservation of mass principle, the internal compartment differential equations can be given as:

$$V_i \frac{dC_i}{dt} = A\left(k_p^{(i)} C_{i-1} + k_p^{(i+1)} C_{i+1} - k_p^{(i)} C_i - k_p^{(i+1)} C_i \right), \quad 2 \le i \le n-1$$

(7)

where A is the area of application, V_i is the volume of the i-th compartment and $k_p^{(i)}$ is the permeability coefficient of the sub-membrane between compartment i-1 and i. Generally, the volumes of compartments and the permeability coefficients can be non-identical $\left(\text{i.e. } V_i \ne V_j, k_p^{(i)} \ne k_p^{(j)} \text{ for } i \ne j\right)$, but here we assume that $V_i = V_m/(n+1)$, where V_m is the volume of the membrane. As will be shown later, unequal permeability coefficients can describe a variable diffusion coefficient. Also, the number of internal compartments (n) is a parameter that should be selected from practical considerations, and it should not be higher than the number of corneocyte layers in the SC, which is about 25 [33].

It is not practical to have more than about 4-6 unknown parameters (such as $k_p^{(i)}$) in a model, as determining these parameters from experimental data is problematic. Therefore, $k_p^{(i)}$ must be related to physiologically based parameters, such as diffusion coefficient. One of the ways of achieving this is to make sure that the steady state flux $\left(J_{ss} \right)$ for the compartmental model is equal to that of the diffusion model and all $k_p^{(i)}$ are the same. Therefore, we can impose the following condition on the total resistance of the membrane R:

$$R = \sum_{i=1}^{n+1} \frac{1}{k_p^{(i)}} = \frac{1}{k_p^{(i)}} \sum_{i=1}^{n+1} 1 = \frac{n+1}{k_p^{(i)}} = \frac{h_m}{D_m}$$

Therefore

$$k_p^{(i)} = (n+1) \frac{D_m}{h_m}, \quad 1 \le i \le n+1$$

(8)

As a result, the total permeability of the SC is defined through the sum of resistances of sub-membranes $\left(1/k_p^{(i)}\right)$, where the partitioning coefficient between the donor and membrane is taken into account by:

8

$$k_p^{sc} = K_m \left[\sum_{i=1}^{n+1} \frac{1}{k_p^{(i)}} \right]^{-1} = \frac{K_m D_m}{h_m}$$

(9)

As described in Fig. 1B, the permeability between the donor and the first compartment ($\tilde{k}_p^{(1)}$) and the last compartment and the receptor ($\tilde{k}_p^{(n+1)}$) can be influenced by donor-stratum corneum interfacial resistance ($1/k_p^d$) and the unstirred aqueous diffusion layer in the viable epidermis- ($1/k_p^{ve}$) respectively. Therefore, these permeability coefficients are defined as:

$$\tilde{k}_p^{(1)} = \left[\frac{1}{k_p^{(1)}} + \frac{K_m}{k_p^d} \right]^{-1} = \frac{k_p^{(1)}}{1+(n+1)\kappa_d^{-1}} = \frac{(n+1)}{1+(n+1)\kappa_d^{-1}} \left(\frac{D_m}{h_m} \right)$$

(10)

$$\tilde{k}_p^{(n+1)} = \left[\frac{1}{k_p^{(n+1)}} + \frac{K_m}{k_p^{ve}} \right]^{-1} = \frac{k_p^{(n+1)}}{1+(n+1)\kappa_{ve}^{-1}} = \frac{(n+1)}{1+(n+1)\kappa_{ve}^{-1}} \left(\frac{D_m}{h_m} \right)$$

(11)

where $\kappa_d = k_p^d / k_p^{sc}$ is the relative permeability of the donor-stratum corneum interfacial resistance, and $\kappa_{ve} = k_p^{ve} / k_p^{sc}$ is the relative permeability of the unstirred aqueous diffusion layer in the viable epidermis in [23]. Thus, the compartmental model equations are:

$$\frac{dC_d}{dt} = \frac{1}{V_{dN} t_d} \left(\frac{n+1}{1+(n+1)\kappa_d^{-1}} \left(\frac{1}{K_m} C_1 - C_d \right) - \kappa_{ev} C_d \right)$$

(12)

for donor compartment,

$$\frac{dC_1}{dt} = \frac{n(n+1)}{t_d} \left(\frac{1}{1+(n+1)\kappa_d^{-1}} (K_m C_d - C_1) + C_2 - C_1 \right)$$

(13)

for the first SC compartment,

$$\frac{dC_i}{dt} = \frac{n(n+1)}{t_d} (C_{i-1} + C_{i+1} - 2 C_i), \quad i = 2,\ldots,n-1$$

(14)

for all SC internal compartments. The equation for the last SC compartment:

9

$$\frac{dC_n}{dt} = \frac{n(n+1)}{t_d}\left(C_{n-1} - C_n + \frac{1}{1+(n+1)\kappa_{ve}^{-1}}\left(\frac{K_m}{K_r}C_r - C_n\right)\right)$$

(15)

while the equation for receptor compartment is:

$$\frac{dC_r}{dt} = \frac{1}{V_{rN}t_d}\left(\frac{n+1}{1+(n+1)\kappa_{ve}^{-1}}\left(\frac{K_r}{K_m}C_n - C_r\right) - Cl_{rN}C_r\right)$$

(16)

where $t_d = h_m^2/D_{m0}$, $\kappa_{ev} = Cl_{ev}/(A\,k_p^{sc})$, $V_{dN} = V_d/(V_m\,K_m)$, $V_{rN} = V_r\,K_r/(V_m\,K_m)$ and

$Cl_{rN} = Cl_r\,K_r/(A\,k_p^{sc})$ are the characteristic time of diffusion through a membrane, dimensionless parameter describing ratio of the rate of solute evaporation to the rate of the solute absorption, donor volume number, receptor volume number, and the dimensionless removal rate from the receptor phase, respectively [23].

Therefore, the flux can be given as:

$$J(t) = \left(C_n(t) - \frac{K_m}{K_r}C_r(t)\right)\tilde{k}_p^{(n+1)}$$

(17)

and the total amount of solute absorbed in receptor phase is:

$$Q(t) = A\int_0^t J(\tau)d\tau$$

(18)

Notably, when there is no donor-SC interfacial resistance, the unstirred aqueous diffusion layer in the viable epidermis i.e. $(\kappa_d, \kappa_{ve} \rightarrow \infty)$ and the sink condition applies in the receptor compartment $(C_r(t) = 0)$, the Equations (12)-(15) are identical to those previously published [10]. Furthermore, the compartmental model equations of the constant concentration donor system can be solved analytically for $Q(t)$ with any number of compartments (n) as:

$$Q(t) = Q_\infty\left[\frac{t}{t_d} - \frac{1}{n}\sum_{i=1}^n\left(\frac{1-e^{a\,r_i\,t}}{r_i^2\,P_i}\right)\right]$$

(19)

where $Q_\infty = k_p^{sc} A C_{d0} t_d$, P_i, r_i, and a are given as:

$$P_j = \prod_{i=1}^{n} \left(r_j - r_i + \delta_{ij} \right)$$

(20)

$$r_i = -2 + 2\cos\left(\frac{i\pi}{n+1} \right), \text{ for } i = 1, \ldots, n$$

(21)

$a = n(n+1)/t_d$ and symbol δ_{ij} is the Kronecker delta function $\left(\delta_{i=j} = 1, \text{ and } \delta_{i \neq j} = 0 \right)$. The derivation of Equation (19) is consistent with published work by Noschese et al. [34] in the applications of eigenvalues of special types of matrices.

Equations (13)-(15) with C_d and C_r set to zero can be used to describe the desorption of solute from the membrane [35, 36]. In this case the membrane is initially saturated with the solute, so the initial conditions are $C_i(0) = K_m C_0$ for $i = 1, \cdots, n$, where $K_m C_0$ refers to the initial concentration in the membrane. Also, the resultant ordinary differential equations can be solved analytically.

A diagrammatic approach can be used to represent Equations (12)-(16) as a flowchart, which can be used in STELLA or Berkeley Madonna to perform simulations (Fig. 2).
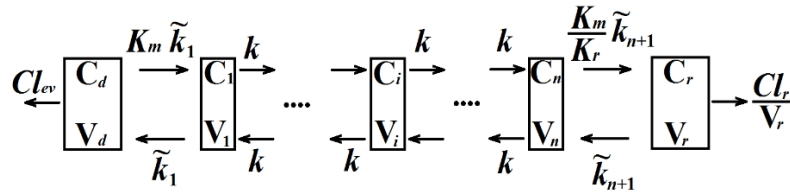

Figure 2. Diagrammatic approach for the compartmental equations, where the parameters are defined as: $k = n(n+1)/t_d$, $\tilde{k}_1 = \alpha k$, $\tilde{k}_{n+1} = \beta k$, $\alpha = 1/\left(1+(n+1)\kappa_d^{-1}\right)$, $\beta = 1/\left(1+(n+1)\kappa_{ve}^{-1}\right)$ and $V_i = A h_m / n$.

Diffusion coefficient as a function of concentration

In percutaneous solute penetration scenarios, using a penetration enhancer is an example of a model with a diffusion coefficient as a function of concentration [29]. In this case, Equation (1) should be rewritten as [37-40]:

$$\frac{\partial C_m}{\partial t} = \frac{\partial}{\partial x}\left(D_m\left(C_m\right)\frac{\partial C_m}{\partial x}\right)$$

(22)

Finding a closed form solution of the Equation (22) [41] or even numerical solution [42, 43] is a challenging task. For example, solving a nonlinear partial differential equation such as Equation (22) can be done numerically using different sophisticated methods such as the finite difference method [44], or the finite element method (FEM) [45]. However, the present compartmental approach can be used for modeling the variable diffusion coefficient by modifying Equation (8) for $k_p^{(i)}$ to take $D_m\left(C_m\right)$ into account. The diffusion coefficient $D_m\left(C_m\right)$ can be represented as:

$$D_m\left(C_m\right) = D_{m0}\, F\left(C_m\right)$$

(23)

where D_{m0} is the diffusion coefficient when the concentration of the solute in the membrane approaches zero, and dimensionless $F\left(C_m\right)$ (where $F(0) = 1$) is an explicit form of the diffusion coefficient as a function of the membrane concentration, which will be specified later. Equation (23) needs to be substituted into Equations (8), (10) and (11) with the concentration (C_m) replaced by the concentration in the appropriate compartment to find permeability coefficients between compartment, yielding:

$$\tilde{k}_p^{(1)} = \left[\frac{1}{k_p^{(1)}} + \frac{K_m}{k_p^d}\right]^{-1} = \left[\frac{1}{(n+1)\,F\left(K_m C_d\right)}\frac{h_m}{D_{m0}} + \frac{K_m}{k_p^d}\right]^{-1} = \frac{(n+1)\,F\left(K_m C_d\right)}{1+(n+1)\,F\left(K_m C_d\right)\kappa_d^{-1}}\frac{D_{m0}}{h_m} \quad (24)$$

$$k_p^{(i)} = (n+1)\,F\left(C_{i-1}\right)\frac{D_{m0}}{h_m}, i = 2,\cdots,n \tag{25}$$

$$\tilde{k}_p^{(n+1)} = \left[\frac{1}{k_p^{(n+1)}} + \frac{K_m}{k_p^{ve}}\right]^{-1} = \left[\frac{1}{(n+1)\,F\left(C_n\right)}\frac{h_m}{D_{m0}} + \frac{K_m}{k_p^{ve}}\right]^{-1} = \frac{(n+1)\,F\left(C_n\right)}{1+(n+1)\,F\left(C_n\right)\kappa_{ve}^{-1}}\frac{D_{m0}}{h_m} \quad (26)$$

In these equations $\kappa_d = k_p^d h_m / (D_{m0} K_m)$ and $\kappa_{ve} = k_p^{ve} h_m / (D_{m0} K_m)$.

Numerically solving differential equations with concentration dependent coefficients is a relatively straightforward (see Appendix A) procedure, reflecting the flexibility of the new approach to accommodate concentration dependent diffusion coefficient.

Various explicit forms of $D_m(C)$ have been reported [37, 44, 46-49], in this work the exponential form will be considered: $D_m(C) = D_{m0}\, e^{\beta C}$, where β is a constant with the unit of reciprocal concentration. The total flux of the solute into the receptor compartment becomes:

$$J(t) = \left(C_n(t) - \frac{K_m}{K_r} C_r(t)\right) \frac{(n+1)\, e^{\beta\, C_n(t)}}{1 + (n+1)\, e^{\beta\, C_n(t)}\, \kappa_{ve}^{-1}} \frac{D_{m0}}{h_m}$$

(27)

where $C_n(t)$, and $C_r(t)$ can be calculated numerically (see Appendix A). The total amount of solute ($Q(t)$) can then be found using Equation (18).

Reduction of donor volume due to evaporation

Solute evaporation from the finite volume donor was previously considered [10, 50]. However, only the constant donor volume which is unaffected by evaporation was considered, so that the Laplace technique can be applied [10]. The new compartmental approach allows us to address the scenario where the volume of the donor reduces due to solvent evaporation of the donor phase. For this case, Equation (5) has to be modified to take the variation of donor volume into account:

$$\frac{d}{dt}\left(V_d(t) C_d(t)\right) = A D_m \left.\frac{\partial C_m(x,t)}{\partial x}\right|_{x=0} - Cl_{ev} C_d(t)$$

(28)

$V_d(t)$ can be expressed as:

$$V_d(t) = V_{d0} v(t)$$

(29)

where V_{d0} is the volume of the donor at $t = 0$, and $v(t)$ determines the relative rate of solvent evaporation, which can be obtained from experiments. Substituting Equation (29) in (28) yields after some algebra:

$$\frac{dC_d}{dt} = \frac{1}{V_{dN} \, t_d \, v(t)} \left(\frac{n+1}{1+(n+1)\kappa_d^{-1}} \left[\frac{1}{K_m} C_1 - C_d \right] - \left(\kappa_{ev} + V_{dN} \, t_d v'(t) \right) C_d \right)$$

(30)

where $v'(t) = dv/dt$. Combining Equation (30) with Equations (13)-(16) yields the compartmental approach for the finite donor volume with evaporation of the solvent in the donor phase, and this emphasizes the flexibility of the new approach to include evaporation scenario only by modifying equation of the donor compartment.

As an example, an exponential reduction in the donor volume due to the solvent evaporation process will be considered. Such a scenario is reasonable when a volatile part of the donor phase evaporates. In this case $V_d(t)$ can be presented as:

$$V_d(t) = V_d^{(nv)} + V_d^{(v)} \, e^{-k_{se}t}$$

(31)

where $V_d^{(nv)}$ is the volume of the non-volatile part of the donor, $V_d^{(v)}$ is fraction of volume reduction due to evaporation, and parameter k_{se} is related to the rate of solvent evaporation. Substituting Equations (31) and (29) in (30) yields:

$$\frac{dC_d}{dt} = \frac{1}{t_d \left(V_{dN}^{(nv)} + V_{dN}^{(v)} e^{-k_{se}t} \right)} \left(\frac{n+1}{1+(n+1)\kappa_d^{-1}} \left[\frac{1}{K_m} C_1 - C_d \right] - \left(\kappa_{ev} - k_{se} \, t_d \, V_{dN}^{(v)} e^{-k_{se}t} \right) C_d \right) \quad (32)$$

where dimensionless donor volume number of non-volatile and volatile parts are $V_{dN}^{(nv)} = V_d^{(nv)} / (K_m V_m)$ and $V_{dN}^{(v)} = V_d^{(v)} / (K_m V_m)$ respectively.

Miller and Kasting [51] modelled simultaneous absorption and evaporation from a multicomponent formulation applied to skin and developed a spreadsheet-based computer program using the diffusion model with finite difference approach. It should be possible to extend the compartment model to include multicomponent formulations, but is believed to be beyond the scope of this paper.

Simulations and Data Analysis

The experimental SC water penetration data from previous work [36] was used. Compartmental model numerical simulations were performed using *ode23s* solver in MATLAB. The numerical simulations of the diffusion PDE were performed using COMSOL Multiphysics®. Talbot method [52] implemented in MATLAB was used for inverting Laplace transformations numerically to calculate $J(t)$, $Q(t)$ and $C_r(t)$ [23, 24].

Results and Discussion

Constant concentration donor: Experimental data for Percutaneous water penetration

In Fig. 3 experimental data for water penetrating the SC [36] were fitted by compartmental and diffusion models. For the diffusion model, the cumulative amount absorbed was taken as $\hat{Q}(s) = k_p^{sc} A C_{d0} t_d \sqrt{s t_d} \big/ \left(s^2 t_d \sinh \sqrt{s t_d} \right)$ [53], and the compartmental model $Q(t)$ was found by numerically solving compartmental equations together with Equation (19). The fitted parameters using nonlinear regression in the compartmental model, which are in this case the characteristic diffusion time t_d and the steady state flux J_{ss}, have been calculated for a different number of compartments. Graphically, it can be seen from Fig. 3A-C that all models provide a good quality of fit. However, the regression quality for the compartmental model with 3 compartments is noticeably better for the first 30 minutes than for the diffusion model and compartmental models with higher number of compartments (see Fig. 3 A). Table 1 provides the results obtained for the fitted parameters and the summary regression statistics. It can be seen from the table that the compartmental model with 3 compartments produces the highest value for MSC (model selection criterion [54], parameter similar to the Akaike information criterion [55, 56]). This result indicates that even for a small number of compartments the compartmental model has a potential to fit some data better than the simple diffusion model. However, applying slow binding model [36], and therefore explicitly accounting for a slow binding/partitioning process in the transport through SC, improves the fitting quality (Table 1) compared to simple diffusion model. Such direct inclusion of transport processes is evidently superior and we plan to explicitly include slow binding/partitioning to the compartmental approach in the future.
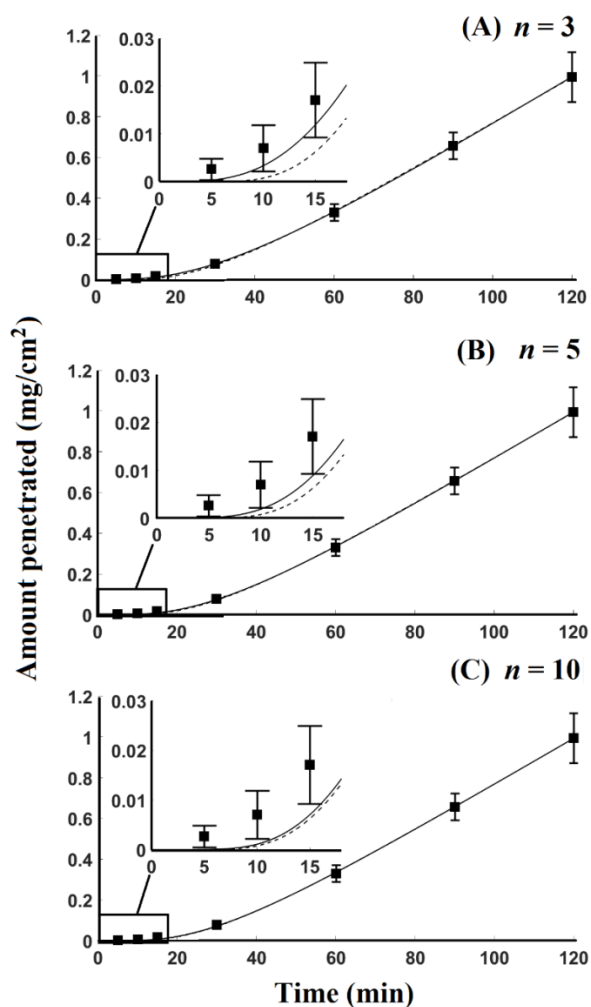
Figure 3. Experimental data for water penetration profiles in SC (■) and their regression profiles for diffusion model (– –) and compartmental model (—) with (A) three, (B) five, and (C) ten compartments.

Table 1. The results of fitting using compartmental and diffusion models

Compartmental Model (n)	t_d (min)	J_{ss} ($\mu g/(cm^2\,min)$)	Model Selection Criteria
3	165 ± 3.5	11.6 ± 0.12	9.02
5	170 ± 4.9	11.4 ± 0.16	8.26
10	178 ± 6.1	11.3 ± 0.18	7.83
1000	192 ± 7.1	11.3 ± 0.2	7.66
Diffusion model [53]	192 ± 7.1	11.3 ± 0.2	7.66
Slow Binding model [36][*]	166.5 ± 4.9	11.5 ± 0.2	8.23

Comparisons with the diffusion model

Anissimov and Roberts solved Equations (3)-(6) for constant concentration donor and finite vehicle volume systems using Laplace domain solutions [23, 24]. In Fig. 4, fluxes for the compartmental model with $n = 3$, and 10 and the diffusion model for selected values of $\kappa_{ve}, \kappa_d, V_{rN}$ and Cl_{rN} are presented for infinite donor volume. It can be seen from Fig. 4 that both models reach the same steady state flux value, as expected. Also, Fig. 4A-C shows that there are slight differences between models especially in the early stage with three compartments, whereas the impact of these differences is negligible for ten compartments, and this agrees with Fig. 3C. However, as shown in Fig. 4D, when the total resistance is mainly caused by the SC i.e. $\kappa_{ve} = \kappa_d \to \infty$, the deviation between the models is significant.
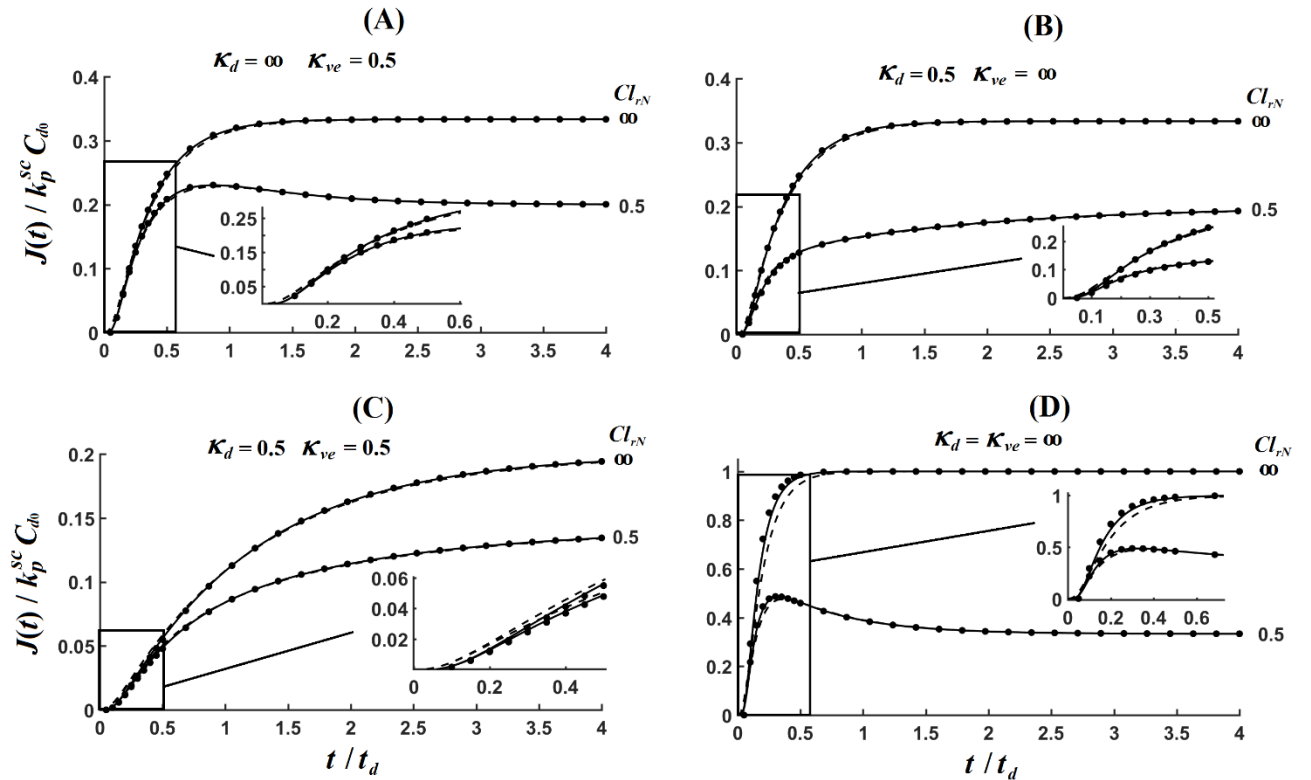

Figure 4. Comparison between normalized flux calculated by diffusion model (●) and compartmental model $n = 3$ (dashed lines), and $n = 10$ (solid lines) for $\left(V_{rN} = 0.5, Cl_{rN} = 0.5, \infty \right)$ versus normalized time $\left(t/t_d \right)$; (A) absence of vehicle-SC resistance; (B) absence of epidermal resistance; (C) effect of epidermal and vehicle-SC resistance; (D) absence of epidermal and vehicle-SC resistance.

The differences between the diffusional and compartmental models (with n = 3, 5, and 10 compartments) can be investigated by considering the maximum relative difference between the models for normalized flux $\left(\delta \bar{J}\right)$ and relative difference for peak flux $\left(\Delta J_{\text{peak}}\right)$ as:

$$\delta \bar{J} = \frac{\left| \bar{J}\left(t_{\text{max}}\right)_{diffusion} - \bar{J}\left(t_{\text{max}}\right)_{compartment} \right|}{\bar{J}\left(t_{\text{max}}\right)_{diffusion}} \times 100\ \%$$

(33)

$$\Delta J_{\text{peak}} = \frac{\left| \left(J_{\text{peak}}\right)_{diffusion} - \left(J_{\text{peak}}\right)_{compartment} \right|}{\left(J_{\text{peak}}\right)_{diffusion}} \times 100\ \%$$

(34)

where t_{max} is the moment when $\left| \bar{J}\left(t\right)_{diffusion} - \bar{J}\left(t\right)_{compartment} \right|$ reaches maximum value. Experimentally measuring the flux of a substance at a very early time is often not possible or imprecise, as the concentration in the receptor compartment is very low; therefore, the comparison between models for $\delta \bar{J}$ will only be considered for times when $t \geq 0.15\, t_{\text{peak}}$, where t_{peak} is the time to reach the maximum flux. Notably, in the constant concentration donor system $J_{\text{peak}} \geq J_{ss}$, and for $J_{\text{peak}} = J_{ss}$ the relative difference for peak flux is zero. While varying the parameters κ_d, κ_{ve}, V_{rN}, and Cl_{rN} independently over the set of values $\{0.5, 1, 2, 4, \infty\}$ in Equations (33) and (34), the derived median values of $\delta \bar{J}$ for n = 3, 5, and 10 compartments are 45%, 19%, and 7% respectively, whereas the median values of ΔJ_{peak} are 1.4%, 0.8% and 0.3% respectively. As expected, there is a clear decreasing trend in both $\delta \bar{J}$ and ΔJ_{peak} with the increase in the number of compartments.

In the finite vehicle volume, varying κ_d, κ_{ve}, V_{rN}, V_{dN} and Cl_{rN} independently over the set of values $\{0.5, 1, 2, 4, \infty\}$ in Equations (33) and (34), the derived median values of $\delta \bar{J}$ for n = 3, 5 and 10 compartments are 49%, 21% and 7% respectively, whereas the median values for ΔJ_{peak} are 1.4%, 0.7% and 0.3% respectively. Thus, the compartmental model deviation from the diffusion model, in both finite vehicle volume and constant concentration donor, reduces with the increase of the number of compartments.

Diffusion coefficient as a function of concentration

Fig. 5 shows the flux for finite volume donor when the diffusion coefficient is exponentially dependent on concentration. Calculations were performed for $V_{dN} = 1$ and $\beta C_{d0} = 0, 1, 5$ for compartmental and diffusion models.
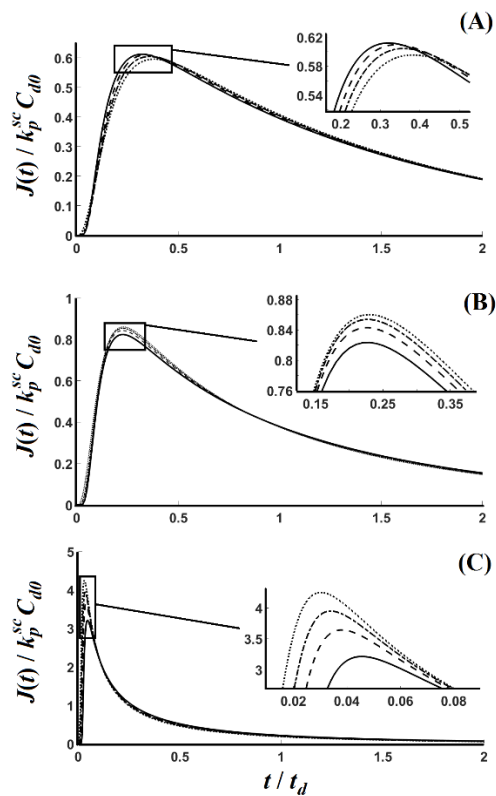

Figure 5. Normalized flux calculated by diffusion (solid lines) and compartmental models with $n = 3$ (dotted lines), 5 (dash dotted lines) and 10 (dashed lines) versus the normalized time profiles (t/t_d) for $D_m(C) = D_{m0}\, e^{\beta C}$; (A) $\beta C_{d0} = 0$; (B) $\beta C_{d0} = 1$; (C) $\beta C_{d0} = 5$.

Fig. 5 shows that the flux for compartmental model approaches that of the diffusion model as the number of compartments increases. It can be seen that a difference between models in terms of peak flux (J_{max}) and peak time (τ_{max}) reduces with the number of compartments.
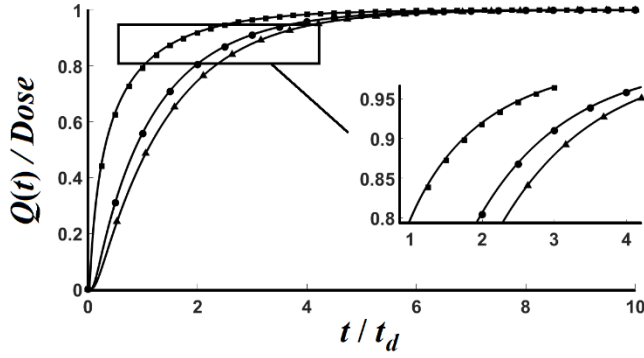
Figure 6. Cumulative amount absorbed calculated by the compartmental model with ($n = 25$ —) and diffusion model ($\blacktriangle \blacktriangle \blacktriangle$ $\beta\, C_{d0} = 0$; $\bullet\bullet\bullet$ $\beta\, C_{d0} = 1$; $\blacksquare\blacksquare\blacksquare$ $\beta\, C_{d0} = 5$) versus normalized time profile (t/t_d) for $V_{dN} = 1$.

Fig. 6 shows a cumulative amount absorbed for the diffusion model and compartmental model with 25 compartments. It can be seen that the difference between the models is negligible when large number of compartments are considered. Notably, increasing the parameter β reduces the time when 90% of the dose is absorbed through the SC. This is expected, as β describes the rate of increase of the diffusion coefficient, and thus the rate of permiation, with the icrease in concentration.

Reduction of vehicle volume due to solvent evaporation

In Fig. 7, the normalized flux $J(t)$ is plotted versus normalized time (t/t_d) for the following parameters: $\kappa_d, \kappa_{ve}, V_{rN}, Cl_{rN} \to \infty, \kappa_{ev} = 0$, and two different values of $k\, t_d = 1$, and 5, which describe different rates of solvent evaporation. Fig. 7 illustrates that for the higher value of solvent evaporation ($k\, t_d = 5$) the higher values of flux are achieved. This is expected, as the concentration in the donor phase would be higher when the donor volume reduces faster due to the faster solvent evaporation. In addition, as in previous cases, the compartmental model predictions approach rapidly to that of the diffusion model with the increase in the number of compartments.
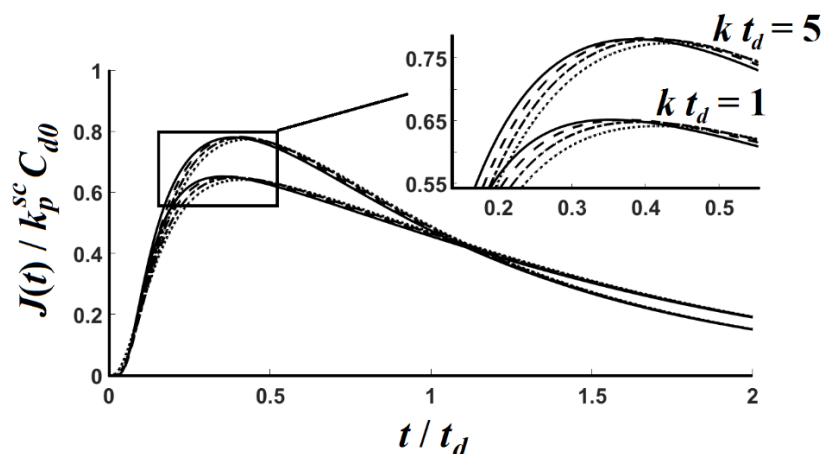
20

Figure 7. Normalized flux calculated by diffusion model using FEM approach (solid lines) and compartmental model with $n=($3 dotted lines, 5 dash dotted lines, 10 dashed lines) versus normalized time profile (t/t_d) for the case where solvent evaporates exponentially with $V_{dN}=1$; $V_{dN}^{(nv)}=0.5$; $V_{dN}^{(v)}=0.5$.

Conclusion

In this work, a new compartmental model describing solute transport in the SC has been developed. The present model offers a simplified approach for modeling a wide variety of exposure scenarios in percutaneous drug delivery systems, including the simulation of skin transport processes in transdermal drug delivery systems with a finite volume donor. The results were in good agreement with the diffusion model. The mathematical flexibility of the new approach should be easily expandable to include modelling transport in different skin layers. In addition, our study provides a flexible framework for assessing performance characteristics of various TDDS. In summary, the present compartmental approach is a relatively simple technique with wide ranging applicability to solving problems related to transport phenomena in skin and other membranes.

Acknowledgements

Appendix A

The compartmental model equations with a diffusion coefficient as a function of concentration can be given, after substituting $k_p^{(i)} = (n+1) D_{m0} F(C_{i-1})/h_m$ in Equations (12)-(16), as:

Donor compartment:

$$\frac{dC_d}{dt} = \frac{1}{V_{dN} t_d}\left(\frac{(n+1) F(K_m C_d)}{1+(n+1) F(K_m C_d)\kappa_d^{-1}}\left(\frac{C_1}{K_m} - C_d \right) F(K_m C_d) - \kappa_{ev} C_d \right)$$

(A.1)

First SC compartment:

$$\frac{dC_1}{dt} = \frac{n(n+1)}{t_d}\left(\frac{F(K_m C_d)}{1+(n+1) F(K_m C_d)\kappa_d^{-1}}(K_m C_d - C_1) + (C_2 - C_1) F(C_1) \right)$$

(A.2)

All SC internal compartments:

$$\frac{dC_i}{dt} = \frac{n(n+1)}{t_d}\left((C_{i-1} - C_i) F(C_{i-1}) + (C_{i+1} - C_i) F(C_i) \right) \quad ,i = 2,\ldots,n-1$$

(A.3)

Last SC compartment:

$$\frac{dC_n}{dt} = \frac{n(n+1)}{t_d}\left((C_{n-1} - C_n) F(C_{n-1}) + \frac{F(C_n)}{1+(n+1) F(C_n)\kappa_{ve}^{-1}}\left(\frac{K_m}{K_r} C_r - C_n \right) \right)$$

(A.4)

Receptor compartment:

$$\frac{dC_r}{dt} = \frac{1}{V_{rN} t_d}\left(\frac{(n+1) F(C_n)}{1+(n+1) F(C_n)\kappa_{ve}^{-1}}\left(\frac{K_r}{K_m} C_n - C_r \right) - Cl_{rN} C_r \right)$$

(A.5)

Solving the new equations can be done numerically with initial conditions such as $C_d(0) = C_{d0}, C_i(0) = 0, \quad i = 1,\ldots,n$ after the function $F(C_m)$ is specified.

References

[1] T. Garg, G. Rath, A.K. Goyal, Comprehensive review on additives of topical dosage forms for drug delivery, Drug Delivery, 22 (2015) 969-987.

[2] M.R. Prausnitz, S. Mitragotri, R. Langer, Current status and future potential of transdermal drug delivery, Nature Reviews Drug Discovery, 3 (2004) 115-124.

[3] V.P. Shah, Transdermal Drug Delivery System Regulatory Issues, in: J. Hadgraft, R.H. Guy (Eds.) Transdermal drug delivery, Dekker, New York, 2003, pp. 371-377.

[4] J.L. Zatz, Simulation Studies of Skin Permeation, Journal of the Society of Cosmetic Chemists, 43 (1992) 37-48.

[5] M.A. Khanday, A. Rafiq, Numerical Estimation of Drug Diffusion at Dermal Regions of Human Body in Transdermal Drug Delivery System, Journal of Mechanics in Medicine and Biology, 16 (2016).

[6] S. Mitragotri, Y.G. Anissimov, A.L. Bunge, H.F. Frasch, R.H. Guy, J. Hadgraft, G.B. Kasting, M.E. Lane, M.S. Roberts, Mathematical models of skin permeability: an overview, Int J Pharm, 418 (2011) 115-129.

[7] J.E. Riviere, Dermal absorption models in toxicology and pharmacology, in, Taylor & Francis, Boca Raton, 2005, pp. 252-276.

[8] J. Hadgraft, R.H. Guy, Feasibility Assessment in Topical and Transdermal Delivery: Mathematical Models and In Vitro Studies, in: J. Hadgraft, R.H. Guy (Eds.) Transdermal Drug Delivery, Dekker, New York, 2003, pp. 16-38.

[9] R.R. Bhagwat, I.S. Vidhya, Novel drug delivery systems: an overview, International Journal of Pharmaceutical Sciences and Research, 4 (2013) 970-982.

[10] Y.G. Anissimov, Mathematical models for different exposure conditions, in: M.S. Roberts, K.A. Walters (Eds.) Dermal Absorption and Toxicity Assessment, Informa Healthcare, New York, 2008, pp. 271-286.

[11] Y.G. Anissimov, O.G. Jepps, Y. Dancik, M.S. Roberts, Mathematical and pharmacokinetic modelling of epidermal and dermal transport processes, Adv Drug Deliv Rev, 65 (2013) 169-190.

[12] R.L. Bronaugh, H.I. Maibach, Percutaneous absorption : drugs, cosmetics, mechanisms, methodology, 4th ed., Taylor & Francis, Boca Raton, 2005.

[13] M.I. Cabrera, R.J.A. Grau, A generalized integral method for solving the design equations of dissolution/diffusion-controlled drug release from planar, cylindrical and spherical matrix devices, Journal of Membrane Science, 293 (2007) 1-14.

[14] C.M. Groh, M.E. Hubbard, P.F. Jones, P.M. Loadman, N. Periasamy, B.D. Sleeman, S.W. Smye, C.J. Twelves, R.M. Phillips, Mathematical and computational models of drug transport in tumours, J R Soc Interface, 11 (2014) 20131173.

[15] M. Rowland, C. Peck, G. Tucker, Physiologically-based pharmacokinetics in drug development and regulatory science, Annu Rev Pharmacol Toxicol, 51 (2011) 45-73.

[16] K. Godfrey, Compartmental models and their application, Academic Press, London ; New York, 1983.

[17] J.A. Jacquez, Compartmental analysis in biology and medicine, BioMedware, 1996.

[18] M. Holz, A. Fahr, Compartment modeling, Adv Drug Deliv Rev, 48 (2001) 249-264.

[19] K.D. McCarley, A.L. Bunge, Physiologically relevant one-compartment pharmacokinetic models for skin. 1. Development of models, J Pharm Sci, 87 (1998) 470-481.

[20] K.D. McCarley, A.L. Bunge, Physiologically relevant two-compartment pharmacokinetic models for skin, J Pharm Sci, 89 (2000) 1212-1235.

[21] D. Selzer, D. Neumann, U.F. Schaefer, Mathematical models for dermal drug absorption, Expert Opin Drug Metab Toxicol, 11 (2015) 1567-1583.

[22] K. Kubota, H.I. Maibach, A compartment model for percutaneous absorption: compatibility of lag time and steady-state flux with diffusion model, J Pharm Sci, 81 (1992) 863-865.

[23] Y.G. Anissimov, M.S. Roberts, Diffusion modeling of percutaneous absorption kinetics. 1. Effects of flow rate, receptor sampling rate, and viable epidermal resistance for a constant donor concentration, J Pharm Sci, 88 (1999) 1201-1209.

[24] Y.G. Anissimov, M.S. Roberts, Diffusion modeling of percutaneous absorption kinetics: 2. Finite vehicle volume and solvent deposited solids, J Pharm Sci, 90 (2001) 504-520.

[25] W.J. Albery, J. Hadgraft, Percutaneous absorption: theoretical description, J Pharm Pharmacol, 31 (1979) 129-139.

[26] J. Hadgraft, Calculations of drug release rates from controlled release devices. The slab, International Journal of Pharmaceutics, 2 (1979) 177-194.

[27] J. Hadgraft, The epidermal reservoir; a theoretical approach, International Journal of Pharmaceutics, 2 (1979) 265-274.

[28] R.H. Guy, J. Hadgraft, A Theoretical Description Relating Skin Penetration to the Thickness of the Applied Medicament, International Journal of Pharmaceutics, 6 (1980) 321-332.

[29] Y.G. Anissimov, A. Watkinson, Modelling Skin Penetration Using the Laplace Transform Technique, Skin Pharmacology and Physiology, 26 (2013) 286-294.

[30] J. Hadgraft, in: Proceedings of the 29th International Symposium on Controlled Release of Bioactive Materials, Controlled Release Society, 2002, pp. 701-702.

[31] J. Crank, The mathematics of diffusion, 2d ed., Clarendon Press, Oxford, Eng, 1975.

[32] N. Lakshminarayanaiah, Equations of membrane biophysics, Academic Press, Orlando, 1984.

[33] C.S. King, S.P. Barton, S. Nicholls, R. Marks, Change in Properties of the Stratum-Corneum as a Function of Depth, British Journal of Dermatology, 100 (1979) 165-172.

[34] S. Noschese, L. Pasquini, L. Reichel, Tridiagonal Toeplitz matrices: properties and novel applications, Numerical Linear Algebra with Applications, 20 (2013) 302-326.

[35] M.S. Roberts, E.J. Triggs, R.A. Anderson, Permeability of solutes through biological membranes measured by a desorption technique, Nature, 257 (1975) 225-227.

[36] Y.G. Anissimov, M.S. Roberts, Diffusion modelling of percutaneous absorption kinetics: 4. Effects of a slow equilibration process within stratum corneum on absorption and desorption kinetics, J Pharm Sci, 98 (2009) 772-781.

[37] H.L. Frisch, The time lag in diffusion, The Journal of Physical Chemistry, 61 (1957) 93-95.

[38] H. Stenlund, Three methods for solution of concentration dependent diffusion coefficient, Visilab Signal Technologies Oy, Finland, (2011).

[39] H.F. Frasch, A.M. Barbero, Application of numerical methods for diffusion-based modeling of skin permeation, Advanced Drug Delivery Reviews, 65 (2013) 208-220.

[40] A. Naegel, M. Heisig, G. Wittum, Detailed modeling of skin penetration--an overview, Adv Drug Deliv Rev, 65 (2013) 191-207.

[41] R. Paul, Solutions of Concentration-Dependent Diffusion Equation, Physics of Fluids, 3 (1960) 905-907.

[42] J.R. Philip, Numerical Solution of Equations of the Diffusion Type with Diffusivity Concentration-Dependent, Transactions of the Faraday Society, 51 (1955) 885-892.

[43] W. Kass, M. Okeeffe, Numerical Solution of Ficks Equation with Concentration-Dependent Diffusion Coefficients, Journal of Applied Physics, 37 (1966) 2377-&.

[44] T. Ahmed, I.V. Belova, G.E. Murch, Finite Difference Solution of the Diffusion Equation and Calculation of the Interdiffusion Coefficient using the Sauer-Freise and Hall Methods in Binary Systems, Procedia Engineering, 105 (2015) 570-575.

[45] J.E. Rim, P.M. Pinsky, W.W. van Osdol, Finite element modeling of coupled diffusion with partitioning in transdermal drug delivery, Annals of Biomedical Engineering, 33 (2005) 1422-1438.

[46] N. Vahdat, V.D. Sullivan, Estimation of permeation rate of chemicals through elastometric materials, Journal of applied polymer science, 79 (2001) 1265-1272.

[47] R. Ash, S.E. Espenhahn, Transport through a slab membrane governed by a concentration-dependent diffusion coefficient III. Numerical solution of the diffusion equation: 'early-time' and 'root t' procedures, Journal of Membrane Science, 180 (2000) 133-146.

[48] K.H. Hsu, A Diffusion-Model with a Concentration-Dependent Diffusion-Coefficient for Describing Water-Movement in Legumes during Soaking, Journal of Food Science, 48 (1983) 618-&.

[49] G. Frenning, M. Stromme, Drug release modeled by dissolution, diffusion, and immobilization, International Journal of Pharmaceutics, 250 (2003) 137-145.

[50] G.B. Kasting, M.A. Miller, Kinetics of finite dose absorption through skin 2: Volatile compounds, Journal of Pharmaceutical Sciences, 95 (2006) 268-280.

[51] M.A. Miller, G.B. Kasting, A Spreadsheet-Based Method for Simultaneously Estimating the Disposition of Multiple Ingredients Applied to Skin, Journal of Pharmaceutical Sciences, 104 (2015) 2047-2055.

[52] J. Abate, W. Whitt, A unified framework for numerically inverting Laplace transforms, Informs Journal on Computing, 18 (2006) 408-421.

[53] D.G. Petlin, M. Rybachuk, Y.G. Anissimov, Pathway Distribution Model for Solute Transport in Stratum Corneum, Journal of Pharmaceutical Sciences, 104 (2015) 4443-4447.

[54] Y.G. Anissimov, M.S. Roberts, A compartmental model of hepatic disposition kinetics: 1. Model development and application to linear kinetics, Journal of Pharmacokinetics and Pharmacodynamics, 29 (2002) 131-156.

[55] J. Powers, Statistical-Analysis of Pharmacokinetic Data, Journal of Veterinary Pharmacology and Therapeutics, 13 (1990) 113-120.

[56] K. Yamaoka, T. Nakagawa, T. Uno, Application of Akaike's information criterion (AIC) in the evaluation of linear pharmacokinetic equations, J Pharmacokinet Biopharm, 6 (1978) 165-175.